

Iron-Only Hydrogenase Active Site Models Containing a Cysteinyl Group Coordinated through Its Sulfur Atom to One Iron Atom of the Diiron Subsite

Li-Cheng Song,^{*[a]} Jian-Hua Ge,^[a] Jing Yan,^[a] Hu-Ting Wang,^[a] Xiang Luo,^[a] and Qing-Mei Hu^[a]

Keywords: Bioinorganic chemistry / Cysteinyl ligand / Electrocatalysis / Dihydrogen evolution / Iron-only hydrogenase

We have developed a simple and convenient method for the synthesis of the first H-cluster models in which a L-cysteinyl group is coordinated to one of the two iron atoms of the diiron subsite through its sulfur atom. This synthetic method includes (i) treatment of the Boc-protected L-cysteine ester Boc-NHCH(CH₂SH)CO₂Et (**1**, Boc = *tert*-butoxycarbonyl) with EtONa to give the L-cysteinyl mercaptide NaSCH₂CH(NH-Boc)CO₂Et (**2**); (ii) further treatment of **2** with [Cp(CO)₂FeI] to produce the metallothioether ligand Cp(CO)₂FeSCH₂CH(NH-Boc)CO₂Et (**3**); and (iii) treatment of the parent diiron complex [Fe₂(μ-SCH₂)₂CH₂(CO)₆] (**4**), [Fe₂(μ-SCH₂)₂N(*t*Bu)(CO)₆] (**5**), or [Fe₂(μ-SCH₂)₂N(C₆H₄OMe-*p*)(CO)₆] (**6**) with Me₃NO·2H₂O followed by ligand **3** to afford the target model compounds [Fe₂(μ-SCH₂)₂CH₂(CO)₅(ligand **3**)] (**7**), [Fe₂(μ-SCH₂)₂N(*t*Bu)(CO)₅(ligand **3**)] (**8**), or [Fe₂(μ-SCH₂)₂N(C₆H₄OMe-*p*)(CO)₅(ligand **3**)] (**9**), respectively. All the new compounds **2**, **3**, and **7–9** have been characterized

by elemental analysis and various spectroscopic techniques. The X-ray diffraction analysis of **8** has confirmed that these models contain a cysteinyl sulfur atom not only coordinated to one Fe atom of the diiron subsite, but also to the Fe atom of the Cp(CO)₂Fe moiety to form the linkage [Fe_{Cp}-(μ-cysteinyl-S)-Fe_{subsite}], which is similar to [Fe_{cubane}-(μ-cysteinyl-S)-Fe_{subsite}] found in natural enzymes. In addition, spectroscopic and electrochemical measurements have further demonstrated that the linkage [Fe_{Cp}-(μ-cysteinyl-S)-Fe_{subsite}] can provide substantial electronic communication between the diiron subsite and the Cp(CO)₂Fe moiety. Under electrochemical conditions, **8** has been shown to be a catalyst for HOAc proton reduction to dihydrogen, and a new type of E*2E2C mechanism for this catalytic reaction is suggested.

(© Wiley-VCH Verlag GmbH & Co. KGaA, 69451 Weinheim, Germany, 2008)

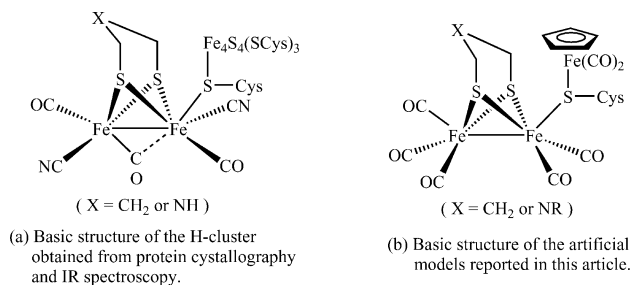
Introduction

Hydrogenases are enzymes, found in many microorganisms, that catalyze both the reduction of protons to dihydrogen and the oxidation of dihydrogen to protons.^[1] These enzymes can be divided into two main groups on the basis of the metals in them: Fe-only hydrogenases^[2,3] and Ni-Fe hydrogenases.^[4–6] In recent years Fe-only hydrogenases (FeHases) have attracted considerably more attention than Ni-Fe hydrogenases, largely because of their unusual structures and particularly because of their catalytic function in the production of the “clean” and highly efficient fuel: dihydrogen.^[7–10] X-ray crystallographic,^[11–14] FTIR spectroscopic,^[15–17] and theoretical^[18] studies revealed that the active site of FeHases, the so-called H-cluster, is composed of a dithiolate-bridged diiron subsite, one of whose iron atoms is linked to a cubane-like Fe₄S₄ cluster through the sulfur atom of the L-cysteinyl group (Scheme 1a). While the diiron subsite catalyzes the formation and activation of di-

hydrogen, the cubic Fe₄S₄ cluster is responsible for electron transfer from and to the active site through the bridging L-cysteinyl group. Inspired by the structural studies of the H-cluster, chemists have synthesized a variety of active site models,^[19,20] and some of them have been found to be catalysts for H/D exchange^[21] and proton reduction to dihydrogen under electrochemical conditions.^[22–24] However, up to now, a H-cluster model in which a cysteinyl group is coordinated through its sulfur atom to one iron atom of the diiron subsite has not appeared in literature, although some cysteinyl-group-containing di- and trinuclear complexes are known.^[25] It should be noted that the synthesis of such a kind of model is particularly of interest, as this provides the possibility of understanding both the biological and chemical functions of the bridging L-cysteinyl group in the H-cluster of FeHases. So, we initiated a study on the synthesis of such model compounds with a basic skeleton structure as shown in Scheme 1b. We introduce the [Cp(CO)₂Fe] moiety into such models in order to replace the complicated cubic Fe₄S₄ cluster and construct the linkage [Fe_{Cp}-(μ-cysteinyl-S)-Fe_{subsite}] for mimicking the [Fe_{cubane}-(μ-cysteinyl-S)-Fe_{subsite}] linkage found in natural enzymes.^[11,12] Thus, in the designed models the cysteinyl sulfur atom is not only coordinated to one iron atom of the diiron subsite,

[a] Department of Chemistry, State Key Laboratory of Elemento-Organic Chemistry, Nankai University, Tianjin 300071, China
Fax: +86-22-23504853
E-mail: lcsong@nankai.edu.cn

but also to the iron atom of the $[\text{Cp}(\text{CO})_2\text{Fe}]$ moiety. Herein we report the first three such biomimetic models with their synthesis, structural characterization, and some properties. In addition, two intermediate products utilized for synthesis of such target model compounds are also described.

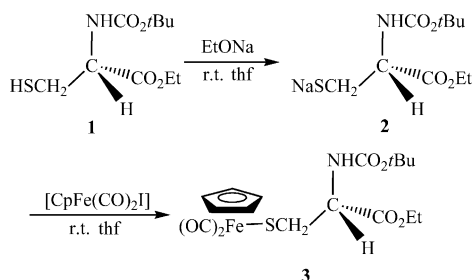


Scheme 1.

Results and Discussion

Synthesis and Spectroscopic Characterization of L-Cysteiny Mercaptide $\text{NaSCH}_2\text{CH}(\text{NH-Boc})\text{CO}_2\text{Et}$ (**2**) and Metallothioether Ligand $\text{Cp}(\text{CO})_2\text{FeSCH}_2\text{CH}(\text{NH-Boc})\text{CO}_2\text{Et}$ (**3**)

According to our designed synthetic method for the target models, we should first prepare new compounds **2** and **3**. As shown in Scheme 2, both **2** and **3** were prepared by starting from the Boc-protected L-cysteine ester $\text{Boc-NHCH}(\text{CH}_2\text{SH})\text{CO}_2\text{Et}$ (**1**, Boc = *tert*-butoxycarbonyl). Treatment of the Boc-protected L-cysteine ester **1** with the freshly prepared EtONa in thf at room temperature gave rise to **2** in a nearly quantitative yield. Then, further treatment of the isolated **2** with $[\text{Cp}(\text{CO})_2\text{FeI}]$ in thf at room temperature or direct treatment of the in situ prepared thf solution of **2** with $[\text{Cp}(\text{CO})_2\text{FeI}]$ at room temperature resulted in formation of **3** in 90% and 94% yields, respectively. Our initial attempt to prepare ligand **3** by direct reaction of **1** with $[\text{Cp}(\text{CO})_2\text{FeI}]$ in the presence of Et_3N was unsuccessful, as indicated by recovery of almost all the starting material $[\text{Cp}(\text{CO})_2\text{FeI}]$. While **2** is a highly hygroscopic white solid, **3** is a slightly air-sensitive red oil. Both **2** and **3** were characterized by elemental analysis and spectroscopy. The IR spectra of **2** and **3** display two absorption bands in the range $1738\text{--}1696\text{ cm}^{-1}$ for their two different organic carbonyl groups, whereas **3** exhibits two additional bands at 2022 and 1968 cm^{-1} resulting from its two terminal

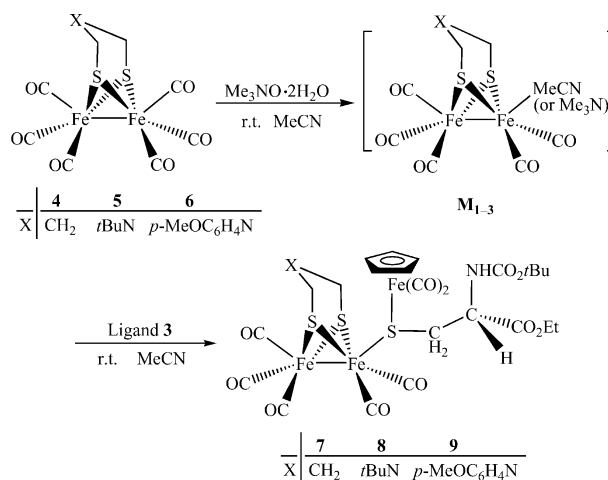


Scheme 2.

carbonyl functions. The ^1H and ^{13}C NMR spectra of **2** and **3** show all the corresponding proton and carbon signals for the Boc-protected L-cysteine ester moiety, whereas **3** displays an additional singlet at $\delta = 4.96\text{ ppm}$ for the five equivalent protons of its Cp ring in its ^1H NMR spectrum and another singlet at $\delta = 85.32\text{ ppm}$ for the five equivalent carbon atoms of its Cp ring in its ^{13}C NMR spectrum.

Synthesis and Spectroscopic Characterization of Target Model Compounds $[\text{Fe}_2(\mu\text{-SCH}_2)_2\text{CH}_2(\text{CO})_5(\text{ligand } 3)]$ (**7**), $[\text{Fe}_2(\mu\text{-SCH}_2)_2\text{N}(t\text{Bu})(\text{CO})_5(\text{ligand } 3)]$ (**8**), and $[\text{Fe}_2(\mu\text{-SCH}_2)_2\text{N}(\text{C}_6\text{H}_4\text{OMe-}p)(\text{CO})_5(\text{ligand } 3)]$ (**9**)

Our target model compounds **7–9** were actually synthesized by the Me_3NO -promoted CO displacement reactions of the parent diiron complexes $[\text{Fe}_2(\mu\text{-SCH}_2)_2\text{CH}_2(\text{CO})_6]$ (**4**), $[\text{Fe}_2(\mu\text{-SCH}_2)_2\text{N}(t\text{Bu})(\text{CO})_6]$ (**5**), and $[\text{Fe}_2(\mu\text{-SCH}_2)_2\text{N}(\text{C}_6\text{H}_4\text{OMe-}p)(\text{CO})_6]$ (**6**) with the above-prepared ligand **3** via the M_{1-3} intermediates,^[26] as shown in Scheme 3. It is noteworthy that ligand **3** should be added after complete consumption of the equimolar mixture of $\text{Me}_3\text{NO}\cdot 2\text{H}_2\text{O}$ and complex **4**, **5**, or **6**, since **3** also contains carbonyl groups that can easily be removed by Me_3NO . In addition, the yields of **8** (45%) and **9** (40%) are much lower than the yield of **7** (80%), presumably because **8** and **9** have much stronger steric repulsion between the bulky ligand **3** and the bulky *t*Bu or *p*-MeOC₆H₄ group at their bridgehead N atom.



Scheme 3.

Model compounds **7–9** are air-stable, brown-black solids, but they are slightly air-sensitive in solution. These compounds were also characterized by elemental analysis and spectroscopic techniques. The IR spectra of **7–9** display two absorption bands in the range $1734\text{--}1713\text{ cm}^{-1}$ for their two different organic carbonyl groups and three absorption bands in the region $2043\text{--}1909\text{ cm}^{-1}$ for their terminal metal carbonyl groups. The ^{13}C NMR spectra of **7–9** each exhibit two signals at ca. 155 and 171 ppm for their two different organic carbonyls; in addition, they display two to four sig-

nals in the range 207–214 ppm for their terminal carbonyl groups. Interestingly, relative to the highest $\nu_{\text{C}=\text{O}}$ frequencies of the parent complexes **4–6**, those corresponding to products **7–9** are shifted by 30–35 cm^{-1} towards lower values (Figure 1). This implies that **3** has a stronger electron-donating influence than CO.^[27] It should be pointed out that the 30–35 cm^{-1} shift is much larger than the ca. 15 cm^{-1} shift of the $\nu_{\text{C}=\text{O}}$ frequencies of the diiron subsite caused by the formal replacement of the Me in the thioether ligand of $[\text{Fe}_2\text{MeC}(\text{CH}_2\text{S})_2(\text{CH}_2\text{SMe})(\text{CO})_5]$ by the cubane dianion, to afford Pickett's model compound $[\text{Fe}_4\text{S}_4\text{L}\{\text{Fe}_2\text{MeC}(\text{CH}_2\text{S})_3(\text{CO})_5\}](\text{NBu}_4)_2$.^[19e] Obviously, this is mainly due to the direct attachment of ligand **3** with the diiron subsite, but the cubane dianion is attached to the diiron subsite by the sulfur atom of the cubane-dianion-containing metalthioether ligand. In addition, it is worth pointing out that such electron-donating influences should be reciprocated in the shifts of the reduction potentials of the diiron subsite in our model compounds **7–9** to more negative potentials, as well as that of the iron atom of ligand **3** in our model compounds **7–9** (vide infra) to a more positive potential.^[19e]

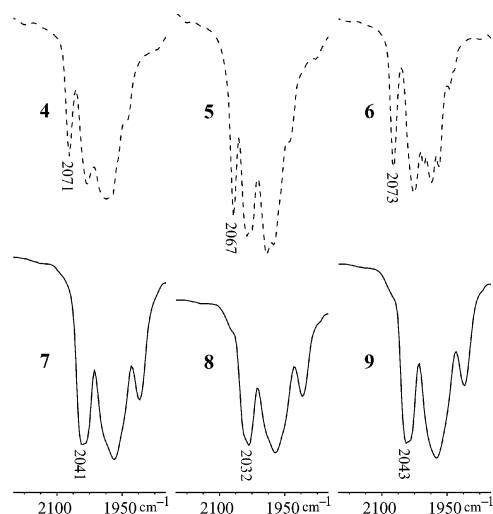


Figure 1. Comparison of the IR spectra of **4–6** with the corresponding spectra of **7–9**.

Crystal Structure of Target Model Compound **8**

The molecular structure of **8** was determined by single-crystal X-ray diffraction techniques. Figure 2 shows its ORTEP plot. Table 1 lists some of its bond lengths and angles. As shown in Figure 2, model compound **8** contains a *tert*-butyl-group-substituted azadithiolate ligand bridged between the two iron atoms of the $\text{Fe}(\text{CO})_3$ and $\text{Fe}(\text{CO})_2$ units to form two fused six-membered rings. The six-membered ring $\text{Fe1-S1-C13-N1-C14-S2}$ has a boat conformation, but another six-membered ring $\text{Fe2-S1-C13-N1-C14-S2}$ adopts a chair conformation. The *tert*-butyl group is equatorially attached to the common nitrogen atom (N1) of the two six-membered rings. Figure 2 also shows that **8** contains a *tert*-butoxycarbonyl-substituted L-cysteiny

group, that is, its C20 has an *R* configuration. This L-cysteiny group is bridged between one iron atom (Fe2) of the diiron subsite and the iron atom (Fe3) of the (dicarbonyl)-cyclopentadienyliron moiety through an *S*-configured sulfur (S3) atom to construct a linkage, $[\text{Fe}_{\text{Cp}}(\mu\text{-cysteiny})\text{S-Fe}_{\text{subsite}}]$, like $[\text{Fe}_{\text{cubane}}(\mu\text{-cysteiny})\text{S-Fe}_{\text{subsite}}]$ found in natural enzymes.^[11,12] The Fe1–Fe2 bond length [2.5255(13) Å] is very close to the corresponding bond lengths in the simple diiron model compounds $[\text{Fe}_2(\mu\text{-SCH}_2)_2\text{CH}_2(\text{CO})_6]$ [2.5103(11) Å],^[28] $[\text{Fe}_2(\mu\text{-SCH}_2)_2\text{NMe}(\text{CO})_6]$ [2.4924(7) Å],^[29] and $[\text{Fe}_2(\mu\text{-SCH}_2)_2\text{O}(\text{CO})_6]$ [2.5113(13) Å],^[30] but they are all slightly shorter than the corresponding bond lengths in the oxidized and reduced DdH hydrogenases (2.60 and 2.55 Å).^[12,13] In addition, the Fe2–S3 bond length [2.3248(16) Å] is shorter than the corresponding bond length (2.5 Å) in the oxidized DdH, but the Fe3–S3 bond length [2.3170(15) Å] is very close to the corresponding bond length (2.3 Å) in the oxidized DdH.^[12]

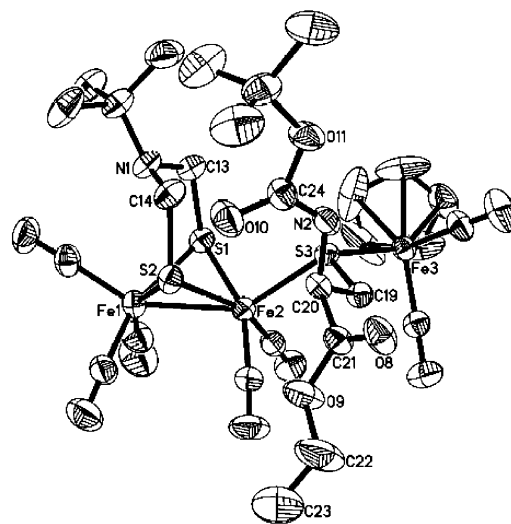


Figure 2. ORTEP view of **8** with 30% probability level ellipsoids.

Table 1. Selected bond lengths [Å] and angles [°] for **8**.

Fe1–S1	2.2614(17)	Fe2–S3	2.3248(16)
Fe1–S2	2.2677(17)	Fe3–S3	2.3170(15)
Fe1–Fe2	2.5255(13)	S3–C19	1.830(5)
Fe2–S1	2.2776(17)	C21–O8	1.199(6)
Fe2–S2	2.2799(16)	C20–N2	1.431(6)
S1–Fe1–S2	84.60(6)	S1–Fe2–Fe1	55.89(5)
S1–Fe1–Fe2	56.50(4)	S2–Fe2–Fe1	56.04(4)
S2–Fe1–Fe2	56.49(4)	S3–Fe2–Fe1	144.30(5)
S1–Fe2–S2	83.95(6)	Fe1–S1–Fe2	67.61(5)
S1–Fe2–S3	99.77(6)	Fe1–S2–Fe2	67.47(5)
S2–Fe2–S3	99.70(6)	Fe3–S3–Fe2	116.26(6)

It is interesting to note that in the unit cell of the crystal structure of **8** (Figure 3) there exists a pair of enantiomers: one is the same as that shown in Figure 2, which contains an *R*-configured C20 and an *S*-configured S3 center, and the other contains an *S*-configured C20A and an *R*-configured S3A center. It is believed that the latter *S/R* isomer was produced from the minor D-cysteiny-group-containing ligand **3**, whereas D-cysteiny ligand **3** was generated from

D-cysteinyl mercaptide **2** and the D-cysteinyl **2** derived from inversion of the *R*-configured C_α of the Boc-protected L-cysteinyl ester **1**. Although some cases are known in which the L-cysteinyl group in L-cysteine ester hydrochlorides keeps its configuration during functional transformation reactions,^[31,32] it is possible to cause some configurational inversion of the C_α atom of **2** from *R* to *S* under basic conditions. This has been proved by the decrease in the specific rotation from the originally prepared **1** ($[\alpha]_D^{20} = +20$, $c = 1.1 \text{ g } 100 \text{ mL}^{-1}$, CHCl_3) to **1** ($[\alpha]_D^{20} = +18$, $c = 1.1 \text{ g } 100 \text{ mL}^{-1}$, CHCl_3) obtained by acidification of **2** with HCl. Figure 3 also shows that in the unit cell this pair of enantiomers of **8** are held together by means of the two intermolecular hydrogen bonds $\text{N2-H2}\cdots\text{O8A}$ and $\text{N2A-H2A}\cdots\text{O8}$. The distance between N2 and O8A or N2A and O8 is 2.990 Å, while the bond angle $\text{N2-H2}\cdots\text{O8A}$ or $\text{N2A-H2A}\cdots\text{O8}$ is 146.1°. These geometric parameters are typical of the hydrogen-bonding interactions.^[33]

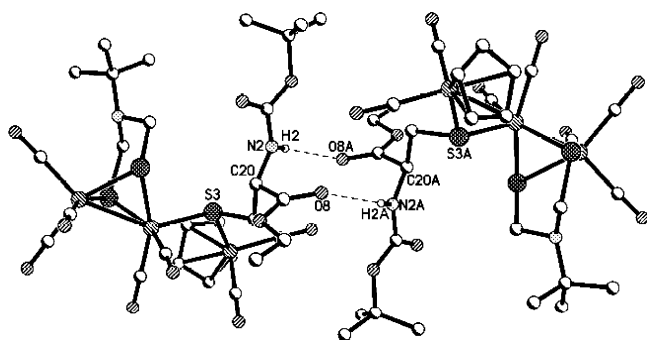


Figure 3. The hydrogen-bonding interaction between two molecules of **8**.

Electrochemistry of Ligand **3**, Model Compound **8**, and Related Complexes

The electrochemical properties of **3** and **8** along with complexes **5** and $[\text{Cp}(\text{CO})_2\text{Fe}]_2$ were determined by CV techniques under identical conditions. Figure 4 shows their cyclic voltammograms, and Table 2 lists their electrochemical data. All the reduction events shown in Figure 4 and Table 2 are one-electron processes, which has been confirmed by bulk electrolysis of **5** (20.7 mmol) at -1.91 V in MeCN. It should be pointed out that for **3** and **8** the irreversible one-electron reduction event at -2.00 V should not be attributed to the reduction of the Fe^{II} atom in **3** and the Fe^{I} atom in **8**, but instead, should be attributed to the reduction of the Fe^{I} atom in $[\text{Cp}(\text{CO})_2\text{Fe}]_2$. It is believed that $[\text{Cp}(\text{CO})_2\text{Fe}]_2$ might be generated from the decomposition of the free ligand **3** or of the coordinated ligand **3** in **8** during the electrochemical process, because it also displays a reduction peak at -2.00 V , and in particular, it has been isolated from the final electrolytic solution of **3** or **8**. In fact, production of $[\text{Cp}(\text{CO})_2\text{Fe}]_2$ is common in CV determinations of the $[\text{Cp}(\text{CO})_2\text{Fe}]$ -containing complexes.^[34] Now, we might assign the first one-electron reduction of **3** at -1.84 V to the reduction of its Fe^{II} atom from Fe^{II} to Fe^{I} , and the first one-electron reduction of **8** at -1.50 V to the

reduction of the Fe^{II} atom in its ligand **3** from Fe^{II} to Fe^{I} . In addition, the second and the fourth reductions at -1.84 and -2.22 V could be assigned to the reduction of the two Fe^{I} atoms in its diiron subsite from $\text{Fe}^{\text{I}}\text{Fe}^{\text{I}}$ to $\text{Fe}^{\text{I}}\text{Fe}^0$ and $\text{Fe}^{\text{I}}\text{Fe}^0$ to Fe^0Fe^0 , respectively. The reduction at -1.84 V might be further assigned to the reduction of the Fe^{I} atom remote from the electron-donating ligand **3**, whereas the reduction at -2.22 V could be ascribed to the reduction of the Fe^{I} atom directly attached to **3**. It follows that the first reduction potential of **8** is positively shifted by 320 mV relative to that (-1.82 V , Table 2) of free ligand **3**, while the second reduction potential at -1.84 V is negatively shifted by 150 mV compared to that (-1.69 V , Table 2) of the parent complex **5**. This is reasonable, since the electron-donating influence of ligand **3** in lowering the $\nu_{\text{C}=\text{O}}$ of the parent complex **5** should be reciprocated in the shifts of the reduction potential of the Fe^{II} atom in ligand **3** to a more positive potential and those of the Fe^{I} atoms in its diiron subsite to more negative potentials, as mentioned above. Finally, it is noteworthy that the 320-mV potential shift is considerably larger than the 120-mV shift caused by the formal replacement of the Me of the thioether ligand in $[\text{Fe}_2\text{MeC}(\text{CH}_2\text{S})_2(\text{CH}_2\text{SMe})(\text{CO})_5]$ by the cubane dianion to give Pickett's model compound.^[19e] The 320- and 150-mV potential shifts, and the 30–35- cm^{-1} $\nu_{\text{C}=\text{O}}$ shifts described above indicate substantial electronic communication occurring in the linkage $[\text{Fe}_{\text{Cp}}-(\mu\text{-cysteinyl-S})-\text{Fe}_{\text{esubsite}}]$ between the diiron subsite and the $[\text{CpFe}(\text{CO})_2]$ unit through the bridging L-cysteinyl group. This electronic communication is apparently more efficient than that occurring in the linkage $[\text{Fe}_{\text{cubane}}-(\mu\text{-SR})-\text{Fe}_{\text{subsite}}]$ of Pickett's model compound.^[19e]

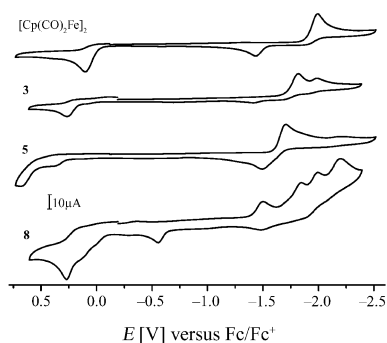


Figure 4. Cyclic voltammograms of **3**, **5**, **8** and $[\text{Cp}(\text{CO})_2\text{Fe}]_2$ (1 mM) in 0.1 M $n\text{Bu}_4\text{NPF}_6/\text{MeCN}$. Scan rate = 100 mV s^{-1} .

Table 2. Redox potentials of **3**, **5**, **8**, and $[\text{Cp}(\text{CO})_2\text{Fe}]_2$ in MeCN at ambient temperature.^[a]

Compound	E^{red} [V]	E^{ox} [V]
$[\text{Cp}(\text{CO})_2\text{Fe}]_2$	-2.00 [b]	0.13 [b]
3	-1.82 [b], -2.00 [b]	0.26 [b]
5	-1.69 [c], -2.20 [b]	0.67 [b]
8	-1.50 [b], -1.84 [b], -2.00 [b], -2.22 [b]	0.27 [b]

[a] MeCN solution (0.1 M $n\text{Bu}_4\text{NPF}_6$) with a glassy carbon working electrode ($A = 0.071 \text{ cm}^2$) referenced to Fc/Fc^+ . Counterelectrode: Pt. Scan rate = 100 mV s^{-1} . [b] Irreversible. [c] Quasi-reversible.

Investigation on Proton Reduction Catalyzed by **8**

We further investigated the electrochemical behavior of **8** in the presence of acetic acid to see whether **8** has the catalytic activity for proton reduction to dihydrogen. As shown in Figure 5, when HOAc was sequentially added from 2 mM to 10 mM, the original peak at -1.50 V did not change, the peak at -1.84 V slightly increased, the peak at -2.00 V disappeared, and the peak at -2.22 V grew dramatically. Obviously, the disappearance of the peak at -2.00 V means that, in the presence of HOAc, **8** became so stable that no $[\text{Cp}(\text{CO})_2\text{Fe}]_2$ was generated. In addition, the continuous increase in the peak at -2.20 V is characteristic of an electrocatalytic process for HOAc proton reduction to dihydrogen catalyzed by **8**.^[22–24,35] Actually, the reduction potential of HOAc with **8** as a catalyst is shifted positively by 400 mV relative to that without **8**. The bulk electrolysis of a MeCN solution of **8** (0.5 mM) with HOAc (25 mM) at -2.25 V indicated that a total of 17.3 F per mol of **8** passed through the electrolysis cell during half an hour. This corresponds to a turnover of 8.7. Gas chromatographic analysis showed that the dihydrogen yield was about 90%.

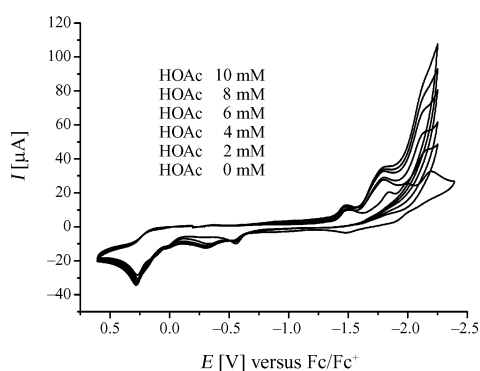
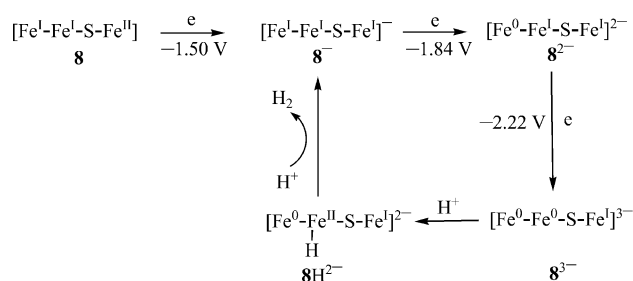


Figure 5. Cyclic voltammograms of **8** (1 mM) with HOAc (2–10 mM) and without HOAc in 0.1 M $n\text{Bu}_4\text{NPF}_6/\text{MeCN}$. Scan rate of 100 mV s^{-1} .

The above-mentioned electrochemical and IR spectral observations, and the previously reported similar cases^[22–24] enable us to propose an E*2E2C (E* represents an electrochemical step outside the catalytic cycle; E and C represent the electrochemical and chemical steps in the catalytic cycle) mechanism to account for H_2 formation from acetic acid catalyzed by **8** (Scheme 4). Firstly, at -1.50 V the Fe^{II} atom of the electron-donating ligand **3** in **8** is preferentially reduced to the Fe^{I} atom to give monoanion $\mathbf{8}^-$. Then, at -1.84 V the Fe^{I} atom remote from **3** in its diiron subsite is reduced to Fe^0 to afford dianion $\mathbf{8}^{2-}$. Thirdly, at -2.22 V the Fe^{I} atom close to **3** in its diiron subsite is reduced to Fe^0 to produce trianion $\mathbf{8}^{3-}$. After one of the Fe^0 atoms in this trianion is protonated by oxidative addition to give species $\mathbf{8H}^{2-}$, it reacts further with another proton to afford the starting monoanion $\mathbf{8}^-$ with H_2 evolution to complete the catalytic cycle. It follows that this E*2E2C mechanism is different from those mechanisms suggested for the simple diiron model complexes, such as **4**,^[36] **6**,^[37] $[\text{Fe}_2(\mu\text{-SCH}_2)_2\text{O}(\text{CO})_6]$,^[30] $[\text{Fe}_2(\mu\text{-SCH}_2)_2\text{CH}_2(\text{CO})_4(\text{CN})(\text{Me}_3\text{P})]$,^[22] and

$[\text{Fe}_2(\mu\text{-SCH}_2)_2\text{CH}_2(\text{CO})_4(\text{Me}_3\text{P})_2]$.^[23] The latter involve only the two Fe^{I} atoms in their diiron subsites, whereas the former E*2E2C mechanism involves not only the two Fe^{I} atoms in its diiron subsite, but also the additional Fe^{II} atom in ligand **3**. It follows that electrocatalytic H_2 production by the E*2E2C mechanism much resembles biological H_2 evolution in natural enzymes, since in enzymes the reductive activation begins with the reduction of the Fe_4S_4 cluster from the 2^+ to the 1^+ state followed by transfer of the reducing equivalent from the Fe_4S_4 cluster to the Fe_2S_2 cluster.^[38] However, it is worthy of note that in the E*2E2C mechanism the reduced $\text{CpFe}(\text{I})(\text{CO})_2$ moiety in **8** does not really transfer the reducing equivalent to the Fe_2S_2 cluster, but controls the reducing order of the two Fe atoms in the Fe_2S_2 cluster by virtue of its strong electron-donating ability.



Scheme 4. Proposed E*2E2C electrocatalysis mechanism for H_2 production from **8** and HOAc.

Conclusions

We have synthesized the first H-cluster model compounds (**7–9**) in which the L-cysteinyll sulfur atom is bridged between one Fe atom of the diiron subsite and the Fe atom of the $[\text{Cp}(\text{CO})_2\text{Fe}]$ moiety. The synthetic route to **7–9** is simple and convenient; it includes first the synthesis of the intermediate products **2** and **3**, followed by the Me_3NO -induced CO substitution of the parent complex **4**, **5**, or **6** by ligand **3**. The X-ray diffraction analysis of **8** has revealed that these models contain a linkage, $[\text{Fe}_{\text{Cp}}-(\mu\text{-cysteinyll-S})\text{-Fe}_{\text{subsite}}]$, which is similar to $[\text{Fe}_{\text{cubane}}-(\mu\text{-cysteinyll-S})\text{-Fe}_{\text{subsite}}]$ found in natural enzymes. Particularly interesting is that the linkage $[\text{Fe}_{\text{Cp}}-(\mu\text{-cysteinyll-S})\text{-Fe}_{\text{subsite}}]$ in these models has been demonstrated by spectroscopic and electrochemical measurements to provide more efficient electronic communication between the diiron subsite and the $[\text{Cp}(\text{CO})_2\text{Fe}]$ moiety than that provided by the $[\text{Fe}_{\text{cubane}}-(\mu\text{-SR})\text{-Fe}_{\text{subsite}}]$ linkage in Pickett's model compound.^[19e] Additionally, model compound **8** has been shown to have the catalytic ability for proton reduction to dihydrogen in HOAc under electrochemical conditions. To improve the catalytic function for H_2 production, we will further modify the structures of **7–9** by using the other 2e ligands to replace their CO ligands and by using various substituted Cp ligands to replace their Cp ligands. Some of the studies along this line are in progress in our laboratories.

Experimental Section

General Comments: All reactions were carried out by using standard Schlenk and vacuum-line techniques under an atmosphere of nitrogen. Acetonitrile was purified by distillation once from P_2O_5 and then from CaH_2 , while thf was purified by distillation from sodium/benzophenone ketyl. The decarbonylating agent $Me_3NO \cdot 2H_2O$ and $L-HCl \cdot H_2NCH(CH_2SH)CO_2Et$ ($[\alpha]_D^{20} = -11$, $c = 8.0$ g/100 mL, 1 N HCl) used for preparing the Boc-protected L-cysteine ester Boc-NHCH(CH₂SH)CO₂Et ($[\alpha]_D^{20} = +20$, $c = 1.0$ g/100 mL, $CHCl_3$) were available commercially. Boc-NHCH(CH₂SH)CO₂Et,^[31] EtONa,^[39] $[Cp(CO)_2FeI]$,^[40] $[Fe_2(\mu-SCH_2)_2-CH_2(CO)_6]$,^[41] $[Fe_2(\mu-SCH_2)_2N(tBu)(CO)_6]$,^[20a] and $[Fe_2(\mu-SCH_2)_2-N(C_6H_4OMe-p)(CO)_6]$ ^[37] were prepared according to the published procedures. Preparative TLC was carried out on glass plates (26 × 20 × 0.25 cm) coated with silica gel H (10–40 μm). Specific rotation ($[\alpha]_D^{20}$) values were obtained by using a Perkin–Elmer Model 341 polarimeter. IR spectra were recorded with a Bruker Vector 22 infrared spectrophotometer. ¹H (¹³C) NMR spectra were recorded with a Bruker Avance 300 NMR or a Varian Mercury Plus 400 NMR spectrometer. Elemental analyses were performed with an Elementar Vario EL analyzer. Melting points were determined with a Yanaco MP-500 apparatus and were uncorrected.

Preparation of NaSCH₂CH(NH-Boc)CO₂Et (2): A 100-mL three-necked flask fitted with a magnetic stirring bar, a rubber septum, and a nitrogen inlet tube was charged with Boc-NHCH(CH₂SH)CO₂Et (**1**, 0.050 g, 0.20 mmol), thf (10 mL), and the freshly prepared EtONa (0.014 g, 0.20 mmol). The mixture was stirred at room temperature for 10 min, and then solvent was removed under vacuum to leave a residue. After the residue was thoroughly washed with hexane (10 mL), it was dissolved in thf (5 mL) and filtered to remove the insoluble impurity. The solvent was removed to give **2** as a highly hygroscopic white solid. Yield: 0.053 g, 99%; m.p. 170 °C (dec., determined in a sealed capillary tube). ¹H NMR (400 MHz, CDCl₃): $\delta = 1.28$ (t, $J = 7.2$ Hz, 3 H, CH₂CH₃), 1.44 [s, 9 H, C(CH₃)₃], 2.99 (br.s, 2 H, SCH₂), 4.21 (q, $J = 7.2$ Hz, 2 H, OCH₂), 4.49 (br.s, 1 H, CH), 5.37 (br.s, 1 H, NH) ppm. ¹³C NMR (75.5 MHz, CDCl₃): $\delta = 14.28$ (CH₂CH₃), 28.46 [C(CH₃)₃], 35.61 (SCH₂), 53.54 (CH), 61.93 (OCH₂), 80.31 [C(CH₃)₃], 155.29 (NHC=O), 170.70 (CHC=O) ppm. IR (KBr disk): $\tilde{\nu} = 1717$ (s, CHC=O), 1696 (s) (NHC=O) cm⁻¹. C₁₀H₁₈NNaO₄S (271.3): calcd. C 44.27, H 6.69, N 5.16; found C 44.21, H 6.53, N 5.11. $[\alpha]_D^{20} = +1.8$ ($c = 0.74$ g/100 mL, thf).

Preparation of Cp(CO)₂FeSCH₂CH(NH-Boc)CO₂Et (3): Method 1: A 100-mL three-necked flask fitted with a magnetic stirring bar, a rubber septum, and a nitrogen inlet tube was charged with NaSCH₂CH(NH-Boc)CO₂Et (**2**, 0.053 g, 0.20 mmol), thf (10 mL), and $[Cp(CO)_2FeI]$ (0.061 g, 0.20 mmol). The mixture was stirred for 1 h at room temperature. The solvent was removed, and the residue was subjected to TLC with acetone/petroleum ether (v/v = 1:2.5) as eluent. From the main red band, **3** was obtained as a red oil. Yield: 0.077 g, 90%. ¹H NMR (300 MHz, CDCl₃): $\delta = 1.25$ (t, $J = 6.9$ Hz, 3 H, CH₂CH₃), 1.42 [s, 9 H, C(CH₃)₃], 2.47 (br.s, 2 H, SCH₂), 4.18 (q, $J = 6.9$ Hz, 2 H, OCH₂), 4.30–4.33 (m, 1 H, CH), 4.96 (s, 5 H, C₅H₅), 5.46 (br.s, 1 H, NH) ppm. ¹³C NMR (100.6 MHz, CDCl₃): $\delta = 13.96$ (CH₂CH₃), 28.11 [C(CH₃)₃], 33.79 (CpFeSCH₂), 55.29 (CH), 60.93 (OCH₂), 79.28 [C(CH₃)₃], 85.32 (C₅H₅), 155.18 (NHC=O), 171.26 (CHC=O), 213.30 (C=O) ppm. IR (KBr disk): $\tilde{\nu} = 2022$ (s), 1968 (vs, C=O), 1738 (s, CHC=O), 1705 (s) (NHC=O) cm⁻¹. C₁₇H₂₃FeNO₄S (425.1): calcd. C 48.01, H 5.45, N 3.29; found C 47.86, H 5.61, N 3.14. **Method 2:** A 100-mL three-necked flask fitted with a magnetic stirring bar, a rubber septum, and a nitrogen inlet tube was charged with Boc-

NHCH(CH₂SH)CO₂Et (**1**, 0.050 g, 0.20 mmol), thf (10 mL), and the freshly prepared EtONa (0.014 g, 0.20 mmol). After the mixture was stirred for 10 min at room temperature, $[Cp(CO)_2FeI]$ (0.061 g, 0.20 mmol) was added. The new mixture was stirred at room temperature for 1 h. The solvent was removed, and the residue was subjected to TLC with acetone/petroleum ether (v/v = 1:2.5) as eluent. From the main red band, **2** (0.080 g, 94%) was obtained as a red oil.

Preparation of $[Fe_2(\mu-SCH_2)_2CH_2(CO)_6][Cp(CO)_2FeSCH_2CH(NH-Boc)CO_2Et]$ (7): A 100-mL three-necked flask fitted with a magnetic stirring bar, a rubber septum, and a nitrogen inlet tube was charged with $[Fe_2(\mu-SCH_2)_2CH_2(CO)_6]$ (**4**, 0.077 g, 0.20 mmol), $Me_3NO \cdot 2H_2O$ (0.022 g, 0.20 mmol), and MeCN (10 mL). The mixture was stirred at room temperature for 0.5 h. At this point, TLC showed that no $[Fe_2(\mu-SCH_2)_2CH_2(CO)_6]$ was left. To this mixture was added $Cp(CO)_2FeSCH_2CH(NH-Boc)CO_2Et$ (**3**, 0.085 g, 0.20 mmol), and the new mixture was stirred at room temperature for 3 h. The solvent was removed, and the residue was subjected to TLC using acetone/petroleum ether (v/v = 1:4) as eluent. From the main brown band, **7** was obtained as a brown-back solid. Yield: 0.125 g, 80%; m.p. 68–70 °C. ¹H NMR (400 MHz, CDCl₃): $\delta = 1.27$ (t, $J = 6.8$ Hz, 3 H, CH₂CH₃), 1.42 [s, 9 H, C(CH₃)₃], 1.72 (br.s, 1 H, CH₂CHHCH₂), 2.15, 1.85 (2br.s, 4 H, CH₂CH₂CH₂), 2.33 (br.s, 1 H, CH₂CHHCH₂), 2.63 (br.s, 2 H, CpFeSCH₂), 4.19 (q, $J = 6.8$ Hz, 2 H, OCH₂), 4.35–4.41 (m, 1 H, CH), 5.09 (d, $J = 7.6$ Hz, 1 H, NH), 5.23 (s, 5 H, C₅H₅) ppm. ¹³C NMR (100.6 MHz, CDCl₃): $\delta = 14.27$ (CH₂CH₃), 22.85 (CH₂CH₂CH₂), 28.47 [C(CH₃)₃], 30.91 (CH₂CH₂CH₂), 34.22 (CpFeSCH₂), 54.73 (CH), 61.90 (OCH₂), 80.28 [C(CH₃)₃], 87.11 (C₅H₅), 155.46 (NHC=O), 171.08 (CHC=O), 211.42, 211.69 (C=O) ppm. IR (KBr disk): $\tilde{\nu} = 2041$ (vs), 1969 (vs), 1911 (s, C=O), 1734 (s, CHC=O), 1713 (s) (NHC=O) cm⁻¹. C₂₅H₂₉Fe₃NO₁₁S₃ (783.2): calcd. C 38.34, H 3.73, N 1.79; found C 38.50, H 3.71, N 1.76.

Preparation of $[Fe_2(\mu-SCH_2)_2N(tBu)(CO)_6][Cp(CO)_2FeSCH_2CH(NH-Boc)CO_2Et]$ (8): The same procedure as that for **7** was followed, but $[Fe_2(\mu-SCH_2)_2N(tBu)(CO)_6]$ (**5**, 0.089 g, 0.20 mmol) was utilized instead of $[Fe_2(\mu-SCH_2)_2CH_2(CO)_6]$ (**4**). With acetone/petroleum ether (v/v = 3:4) as eluent, **8** was obtained as a brown-back solid. Yield: 0.076 g, 45%; m.p. 55–57 °C. ¹H NMR (300 MHz, CDCl₃): $\delta = 0.93$ [s, 9 H, NC(CH₃)₃], 1.22 (br.s, 3 H, CH₂CH₃), 1.38 [s, 9 H, OC(CH₃)₃], 2.42 (br.s, 2 H, CpFeSCH₂), 2.92–3.15 (2br.s, 4 H, CH₂NCH₂), 4.15 (br.s, 2 H, OCH₂), 4.41–4.42 (m, 1 H, CH), 4.91 (s, 5 H, C₅H₅), 5.42 (br.s, 1 H, NH) ppm. ¹³C NMR (100.6 MHz, CDCl₃): $\delta = 14.30$ (CH₂CH₃), 26.51 [NC(CH₃)₃], 28.46 [OC(CH₃)₃], 34.16 (CpFeSCH₂), 49.19 (CH₂NCH₂), 55.56 (CH), 57.19 [NC(CH₃)₃], 61.40 (OCH₂), 79.74 [OC(CH₃)₃], 85.56 (C₅H₅), 155.41 (NHC=O), 171.69 (CHC=O), 208.14, 211.47, 213.19 (C=O) ppm. IR (KBr disk): $\tilde{\nu} = 2032$ (vs), 1972 (vs), 1909 (s, C=O), 1733 (s, CHC=O), 1715 (s) (NHC=O) cm⁻¹. C₂₈H₃₆Fe₃N₂O₁₁S₃ (840.1): calcd. C 40.02, H 4.32, N 3.33; found C 39.80, H 4.47, N 2.93.

Preparation of $[Fe_2(\mu-SCH_2)_2N(C_6H_4OMe-p)(CO)_6][Cp(CO)_2FeSCH_2CH(NH-Boc)CO_2Et]$ (9): The same procedure as that for **7** was followed, but $[Fe_2(\mu-SCH_2)_2N(C_6H_4OMe-p)(CO)_6]$ (**6**, 0.099 g, 0.20 mmol) was employed in place of $[Fe_2(\mu-SCH_2)_2CH_2(CO)_6]$ (**4**). With acetone/petroleum ether (v/v = 1:2.5) as eluent, **9** was obtained as a brown-back solid. Yield: 0.071 g, 40%; m.p. 50–52 °C. ¹H NMR (400 MHz, CDCl₃): $\delta = 1.28$ (br.s, 3 H, CH₂CH₃), 1.45 [s, 9 H, C(CH₃)₃], 2.51 (br.s, 2 H, CpFeSCH₂), 3.77 (s, 3 H, OCH₃), 4.20–4.40 (m, 7 H, CH₂NCH₂, OCH₂, CH), 4.98 (s, 5 H, C₅H₅), 5.50 (br.s, 1 H, NH), 6.72–6.87 (m, 4 H, C₆H₄) ppm. ¹³C NMR (100.6 MHz, CDCl₃): $\delta = 14.39$ (CH₂CH₃), 28.55 [C(CH₃)₃], 34.22

(CpFeSCH₂), 50.72 (CH₂NCH₂), 55.73 (CH), 55.93 (OCH₃), 62.02 (OCH₂), 80.52 [C(CH₃)₃], 87.12 (C₅H₅), 115.31, 117.37, 118.01, 120.18, 120.23 (C₆H₄), 155.42, (NHC=O), 171.77 (CHC=O), 207.27, 208.08, 211.29, 213.22 (C≡O) ppm. IR (KBr disk): $\tilde{\nu}$ = 2043 (vs), 1974 (vs), 1911 (s), C≡O, 1733 (s, CHC=O), 1715 (s, NHC=O) cm⁻¹. C₃₁H₃₄Fe₃N₂O₁₂S₃ (890.3): calcd. C 41.82, H 3.85, N 3.15; found C 41.85, H 4.07, N 3.19.

X-ray Structure Determination of 8: Single crystals of **8** suitable for X-ray diffraction analysis was grown by slow evaporation of the diethyl ether/hexane solution of **8** at 4 °C. A single crystal of **8** was mounted on a Rigaku MM-007 (rotating anode) diffractometer equipped with Saturn 70CCD. Data were collected at room temperature, by using a confocal monochromator with Mo-K α radiation (λ = 0.71070 Å) in the ω - ϕ scanning mode. Data collection, reduction and absorption correction were performed by the CRYSTALCLEAR program.^[42] The structure was solved by direct methods with the SHELXS-97 program^[43] and refined by full-matrix least-squares techniques (SHELXL-97)^[44] on F^2 . Hydrogen atoms were located by using the geometric method. Details of crystal data, data collections, and structure refinements are summarized in Table 3.

Table 3. Crystal data and structure refinement details for **8**.

Formula	C ₂₈ H ₃₆ Fe ₃ N ₂ O ₁₁ S ₃ ·O(C ₂ H ₅) ₂
M_r [g mol ⁻¹]	914.44
Crystal size [mm]	0.10 × 0.08 × 0.06
Crystal system	triclinic
Space group	$P\bar{1}$
a [Å]	10.349(3)
b [Å]	12.028(4)
c [Å]	18.482(7)
α [°]	103.092(8)
β [°]	101.725(9)
γ [°]	104.146(9)
V [Å ³]	2089.8(12)
Z	2
$\rho_{\text{calcd.}}$ [g cm ⁻³]	1.453
μ [mm ⁻¹]	1.233
$F(000)$	948.00
$2\theta_{\text{max}}$ [°]	54.84
Reflections collected	14731
Independent reflections	8452
Index ranges	-12 ≤ h ≤ 12 -15 ≤ k ≤ 15 -23 ≤ l ≤ 14
Goodness of fit	1.089
R	0.0658
R_w	0.1603
Largest diff peak and hole [e Å ⁻³]	0.562/-0.535

CCDC-648593 (for **8**) contains the supplementary crystallographic data for this paper. These data can be obtained free of charge from The Cambridge Crystallographic Data Centre via www.ccdc.cam.ac.uk/data_request/cif.

Electrolysis of 3 or 8 and Isolation of [Cp(CO)₂Fe]₂ from Electrolytic Solutions: The electrolysis of **3** or **8** was performed on a vitreous carbon rod (A = 2.9 cm²) in a two-compartment, gastight, H-type electrolysis cell equipped with a BAS Epsilon potentiostat. A solution of **3** (0.043 g, 0.10 mmol) in acetonitrile (20 mL) with $n\text{Bu}_4\text{NPF}_6$ (0.1 M) was electrolyzed at -1.90 V under a nitrogen atmosphere. The electrolysis was stopped when the current value decreased to 10% of the initial value (ca. 40 min). At this time, cyclic voltammetry showed that the original peak at -1.82 V disappeared, and thus **3** was completely consumed. The resulting electrolytic

solution was condensed to ca. 5 mL in vacuo, and then diethyl ether (20 mL) was added to yield a brown precipitate. The precipitate was washed thoroughly with diethyl ether. The washings were combined, and then diethyl ether was removed in vacuo to leave a residue. The residue was subjected to TLC with acetone/petroleum ether (1:4 v/v) as eluent. A brown band was developed, from which [Cp(CO)₂Fe]₂ (0.011 g) was obtained as a dark-red solid. ¹H NMR (400 MHz, CDCl₃): δ = 4.78 (s, 10 H, 2C₅H₅) ppm. This value is virtually the same as that (δ = 4.79 ppm) reported for an authentic sample.^[41] In addition, its cyclic voltammogram and cyclic voltammetric data are completely the same as the corresponding values shown in Figure 4 and Table 2, respectively. Similarly, [Cp(CO)₂Fe]₂ (0.009 g) was isolated from the electrolytic solution of **8** (0.084 g, 0.10 mmol) produced under the same electrolytic conditions.

Electrochemistry: A solution of $n\text{Bu}_4\text{NPF}_6$ (0.1 M) in MeCN was used as an electrolyte in all cyclic voltammetric and bulk electrolytic experiments. All measurements were made with a BAS Epsilon potentiostat. Voltammograms were obtained in a three-electrode cell with a glassy carbon working electrode of 3 mm diameter, a platinum counterelectrode, and a Ag/Ag⁺ (0.01 M AgNO₃/0.1 M $n\text{Bu}_4\text{NPF}_6$ in MeCN) reference electrode under a nitrogen atmosphere. The working electrode was polished with 0.05 μm alumina paste and sonicated in water for at least 10 min prior to use. All potentials are quoted against the ferrocene/ferrocenium (Fc/Fc⁺) potential. Bulk electrolytic experiments were run with a glassy carbon rod (A = 2.9 cm²) in a two-compartment, gastight, H-type electrolysis cell containing ca. 20 mL of MeCN. The electrolyses of solutions were carried out under hydrodynamic conditions, by vigorously stirring the solutions to mitigate mass transport complications. Gas chromatography was performed with a Shimadzu Gas Chromatograph GC-9A (column: carbon molecular sieves TDX-1, 2.5 m × 5 mm; column temperature: 40 °C) under isothermal conditions with N₂ as a carrier gas and a thermal conductivity detector.

Acknowledgments

We are grateful to the National Natural Science Foundation of China and the Research Fund for the Doctoral Program of Higher Education of China for financial support.

- [1] a) Y. Nicolet, C. Cavazza, J. C. Fontecilla-Camps, *J. Inorg. Biochem.* **2002**, *91*, 1–8; b) P. Tamagnini, R. Axelsson, P. Lindberg, F. Oxelfelt, R. Wunschiers, P. Lindblad, *Macromol. Mol. Biol. Rev.* **2002**, *66*, 1–20; c) M. W. W. Adams, E. I. Stiefel, *Science* **1998**, *282*, 1842–1843; d) R. Cammack, *Nature* **1999**, *397*, 214–215.
- [2] Y. Nicolet, B. J. Lemon, J. C. Fontecilla-Camps, J. W. Peters, *Trends Biochem. Sci.* **2000**, *25*, 138–143.
- [3] J. W. Peters, *Curr. Opin. Struct. Biol.* **1999**, *9*, 670–676.
- [4] A. E. Przybyla, J. Robbins, N. Menon, H. D. Peck Jr, *FEMS Microbiol. Rev.* **1992**, *88*, 109–135.
- [5] A. Volbeda, J. C. Fontecilla-Camps, *Dalton Trans.* **2003**, 4030–4038.
- [6] E. Garcin, X. Vernede, E. C. Hatchikian, A. Volbeda, M. Frey, J. C. Fontecilla-Camps, *Structure* **1999**, *7*, 557–566.
- [7] J. Alper, *Science* **2003**, *299*, 1686–1687.
- [8] M. Y. Darensbourg, E. J. Lyon, J. J. Smees, *Coord. Chem. Rev.* **2000**, *206–207*, 533–561.
- [9] D. J. Evans, C. J. Pickett, *Chem. Soc. Rev.* **2003**, *32*, 268–275.
- [10] M. W. W. Adams, *Biochim. Biophys. Acta, Bioenerg.*, **1990**, *1020*, 115–145.
- [11] J. W. Peters, W. N. Lanzilotta, B. J. Lemon, L. C. Seefeldt, *Science* **1998**, *282*, 1853–1858.

- [12] Y. Nicolet, C. Piras, P. Legrand, C. E. Hatchikian, J. C. Fontecilla-Camps, *Structure* **1999**, 7, 13–23.
- [13] Y. Nicolet, A. L. De Lacey, X. Vernède, V. M. Fernandez, E. C. Hatchikian, J. C. Fontecilla-Camps, *J. Am. Chem. Soc.* **2001**, 123, 1596–1601.
- [14] B. J. Lemon, J. W. Peters, *Biochemistry* **1999**, 38, 12969–12973.
- [15] A. J. Pierik, M. Hulstein, W. R. Hagen, S. P. Albracht, *Eur. J. Biochem.* **1998**, 258, 572–578.
- [16] A. L. De Lacey, C. Stadler, C. Cavazza, E. C. Hatchikian, V. M. Fernandez, *J. Am. Chem. Soc.* **2000**, 122, 11232–11233.
- [17] Z. Chen, B. J. Lemon, S. Huang, D. J. Swartz, J. W. Peters, K. A. Bagley, *Biochemistry* **2002**, 41, 2036–2043.
- [18] H.-J. Fan, M. B. Hall, *J. Am. Chem. Soc.* **2001**, 123, 3828–3829.
- [19] a) X. Zhao, I. P. Georgakaki, M. L. Miller, J. C. Yarbrough, M. Y. Darensbourg, *J. Am. Chem. Soc.* **2001**, 123, 9710–9711; b) C. A. Boyke, T. B. Rauchfuss, S. R. Wilson, M.-M. Rohmer, M. Bénard, *J. Am. Chem. Soc.* **2004**, 126, 15151–15160; c) E. J. Lyon, I. P. Georgakaki, J. H. Reibenspies, M. Y. Darensbourg, *J. Am. Chem. Soc.* **2001**, 123, 3268–3278; d) M. Razavet, S. C. Davies, D. L. Hughes, J. E. Barclay, D. J. Evans, S. A. Fairhurst, X. Liu, C. J. Pickett, *Dalton Trans.* **2003**, 586–595; e) C. Tard, X. Liu, S. K. M. Bruschi, L. De Gioia, S. C. Davies, X. Yang, L.-S. Wang, G. Sawers, C. J. Pickett, *Nature* **2005**, 433, 610–613; f) L.-C. Song, J. Cheng, J. Yan, H.-T. Wang, X.-F. Liu, Q.-M. Hu, *Organometallics* **2006**, 25, 1544–1547; g) F. I. Adam, G. Hogarth, I. Richards, B. E. Sanchez, *Dalton Trans.* **2007**, 2495–2498.
- [20] a) J. D. Lawrence, H. Li, T. B. Rauchfuss, *Chem. Commun.* **2001**, 1482–1483; b) H. Li, T. B. Rauchfuss, *J. Am. Chem. Soc.* **2002**, 124, 726–727; c) L.-C. Song, Z.-Y. Yang, H.-Z. Bian, Q.-M. Hu, *Organometallics* **2004**, 23, 3082–3084; d) L. Schwartz, G. Eilers, L. Eriksson, A. Gogoll, R. Lomoth, S. Ott, *Chem. Commun.* **2006**, 520–522; e) J. Hou, X. Peng, J. Liu, Y. Gao, X. Zhao, S. Gao, K. Han, *Eur. J. Inorg. Chem.* **2006**, 4679–4686; f) L.-C. Song, M.-Y. Tang, F.-H. Su, Q.-M. Hu, *Angew. Chem. Int. Ed.* **2006**, 45, 1130–1133.
- [21] a) X. Zhao, I. P. Georgakaki, M. L. Miller, R. Mejia-Rodriguez, C.-Y. Chiang, M. Y. Darensbourg, *Inorg. Chem.* **2002**, 41, 3917–3928; b) J. L. Nehring, D. M. Heinekey, *Inorg. Chem.* **2003**, 42, 4288–4292.
- [22] F. Gloaguen, J. D. Lawrence, T. B. Rauchfuss, *J. Am. Chem. Soc.* **2001**, 123, 9476–9477.
- [23] D. Chong, I. P. Georgakaki, R. Mejia-Rodriguez, J. Sanabria-Chinchilla, M. P. Soriaga, M. Y. Darensbourg, *Dalton Trans.* **2003**, 4158–4163.
- [24] J.-F. Capon, F. Gloaguen, P. Schollhammer, J. Talarmin, *Coord. Chem. Rev.* **2005**, 249, 1664–1676.
- [25] a) G. Süss-Fink, T. Jenke, H. Heitz, M. A. Pellinghelli, A. Tiripicchio, *J. Organomet. Chem.* **1989**, 379, 311–323; b) B. Galán, D. Miguel, J. Pérez, V. Riera, *Organometallics* **2002**, 21, 2979–2985; c) C. He, M. Wang, X. Zhang, Z. Wang, C. Chen, J. Liu, B. Åkermark, L. Sun, *Angew. Chem. Int. Ed.* **2004**, 43, 3571–3574.
- [26] F. Gloaguen, J. D. Lawrence, M. Schmidt, S. R. Wilson, T. B. Rauchfuss, *J. Am. Chem. Soc.* **2001**, 123, 12518–12527.
- [27] J. P. Collman, L. S. Hegeudus, J. R. Norton, R. G. Finke, *Principles and Applications of Organotransition Metal Chemistry*, 2nd ed., California University Science Books, Mill Valley, **1987**.
- [28] E. J. Lyon, I. P. Georgakaki, J. H. Reibenspies, M. Y. Darensbourg, *Angew. Chem. Int. Ed.* **1999**, 38, 3178–3180.
- [29] J. D. Lawrence, H. Li, T. B. Rauchfuss, M. Bénard, M.-M. Rohmer, *Angew. Chem. Int. Ed.* **2001**, 40, 1768–1771.
- [30] L.-C. Song, Z.-Y. Yang, H.-Z. Bian, Y. Liu, H.-T. Wang, X.-F. Liu, Q.-M. Hu, *Organometallics* **2005**, 24, 6126–6135.
- [31] J. C. Namyslo, C. Stanitzek, *Synthesis* **2006**, 3367–3369.
- [32] M. D. Threadgill, A. P. Gledhill, *J. Org. Chem.* **1989**, 54, 2940–2949.
- [33] P. A. Kollman, L. C. Allen, *Chem. Rev.* **1972**, 72, 283–303.
- [34] M. Morán, I. Cuadrado, J. Losada, *J. Organomet. Chem.* **1987**, 320, 317–324.
- [35] I. Bhugun, D. Lexa, J.-M. Savéant, *J. Am. Chem. Soc.* **1996**, 118, 3982–3983.
- [36] R. Mejia-Rodriguez, D. Chong, J. H. Reibenspies, M. P. Soriaga, M. Y. Darensbourg, *J. Am. Chem. Soc.* **2004**, 126, 12004–12014.
- [37] L.-C. Song, J.-H. Ge, X.-G. Zhang, Y. Liu, Q.-M. Hu, *Eur. J. Inorg. Chem.* **2006**, 3204–3210.
- [38] A. S. Pereira, P. Tavares, I. Moura, J. J. G. Moura, B. H. Huynh, *J. Am. Chem. Soc.* **2001**, 123, 2771–2782.
- [39] C. S. Marrel, E. E. Dreger, *Organic Syntheses, Coll. Vol. 1*, **1941**, 238–240.
- [40] R. B. King, *Organometallic Syntheses, Transition-Metal Compounds*, Academic Press, New York, **1965**, vol. I.
- [41] D. Seyferth, R. S. Henderson, L.-C. Song, *J. Organomet. Chem.* **1980**, 192, C1–C5.
- [42] CRYSTALCLEAR 1.3.6. Rigaku and Rigaku/MS (2005). 9009 New Trail Dr. The Woodlands TX 77381 USA.
- [43] G. M. Sheldrick, *SHELXS97, A Program for Crystal Structure Solution*; University of Göttingen: Germany, **1997**.
- [44] G. M. Sheldrick, *SHELXL97, A Program for Crystal Structure Refinement*; University of Göttingen: Germany, **1997**.

Received: August 5, 2007

Published Online: November 7, 2007